Analysis of the Near-Ultraviolet Absorption Band of Colchicine and the Effect of Tubulin Binding

Susan Bane Hastie* and Richard P. Rava*,†

Contribution from the Department of Chemistry, University Center at Binghamton, State University of New York, Binghamton, New York 13901. *Received April 14, 1988*

Abstract: The near-ultraviolet absorption spectrum of colchicine from 290 to 420 nm has been examined in a variety of solvents and bound to tubulin by multiple differentiation of the absorption spectra. The absorption band is shown to be comprised of two transitions, which are $\pi-\pi^*$ in nature and of different excited-state character. The energies of the transitions do not correlate with solvent properties such as dipole moment, dielectric constant, or refractive index. The lower energy transition was found to shift to shorter wavelength in solvents capable of donating a hydrogen bond, while the higher energy transition was essentially invariant with solvent properties. MNDO calculations on tropone, a model for the C ring of colchicine, and colchicine support the experimental findings and indicate that the benzene moiety of the A ring makes little contribution to the character of these two transitions. Analysis of the absorption and derivative spectra of colchicine bound to tubulin reveals that the absorption spectrum is altered in a manner that is unique to tubulin binding and not mimicked by solvents. It is proposed that the alteration of the electronic transitions in the near-ultraviolet absorption spectrum of colchicine bound to tubulin is the result of the interaction of the colchicine C ring with a π-system in the colchicine-binding site.

Colchicine, an alkaloid isolated from *Colchicum autumnale*, exerts its major biological effects by binding specifically and with high affinity to tubulin, the major protein component of the cytoskeletal structure known as the microtubule.[1-3] The colchicine–tubulin complex substoichiometrically inhibits normal microtubule assembly, resulting in cessation of cellular microtubule-mediated processes. Colchicine has thus received considerable attention due to its utility as a tool for probing microtubule-dependent events in cell biology.

The mechanism of colchicine binding to tubulin has been studied since tubulin was identified as the locus of colchicine activity in the late 1960s.[4,5] In spite of intensive investigations into the nature of the colchicine–tubulin association,[6-14] a clear picture of the mechanism remains elusive. One difficulty in understanding the essence of this ligand–receptor complex lies in the unique and unusual electronic properties of colchicine free in solution and when bound to tubulin. Bhattacharyya and Wolff first noted the unusual electronic properties of colchicine and the colchicine–tubulin complex.[6] Colchicine displays a broad near-ultraviolet (UV) absorption band centering at 353 nm in aqueous solution. When the absorption spectrum of colchicine was examined in solvents of decreasing dielectric constant, this band was found to shift to longer wavelength, consistent with the expected behavior of a $\pi-\pi^*$ transition. In the tubulin-bound species, however, this band is slightly blue-shifted relative to water.

Other unexplained features of the colchicine–tubulin complex are directly related to the electronic properties of colchicine. Tubulin binding induces a dramatic (>350-fold) enhancement of colchicine fluorescence at 440 nm.[6,15] The fluorescence of the bound species appears unrelated to the polarity of the medium, as unbound colchicine fluorescence is only weakly enhanced by decreasing the dielectric constant of the solvent. The sole condition so far found to mimic tubulin-bound colchicine fluorescence was increasing the viscosity of the medium by dissolving colchicine in glycerol.[16] Even under these conditions and extrapolation of the results to infinite viscosity, less than 60% of the protein bound intensity could be induced.

Perhaps the most puzzling electronic feature of the colchicine–tubulin complex is observed by circular dichroism (CD). Colchicine exhibits a negative CD band centering at 340 nm in aqueous solution that has been shown to arise primarily from the interaction of the tropone C ring with the trimethoxyphenyl A ring.[17] When colchicine is bound to tubulin and unbound colchicine is removed, this CD band is greatly reduced in magnitude and may indeed vanish.[9]

In order to understand the alteration in electronic properties of colchicine when it is bound to tubulin, it is necessary to first understand the electronic states of colchicine itself. In this paper, we will show how multiple differentiation of colchicine absorption spectra can be useful in resolving the individual electronic transitions underlying the broad absorption band. We then discuss the effects of solvent on the second and fourth derivatives of the near-UV absorption band of colchicine. The results indicate that there are two overlapping transitions in the near-UV absorption band of colchicine. These transitions are differentially affected by solvent and are determined to be $\pi-\pi^*$ in character. Semiempirical MNDO calculations of colchicine allow an understanding of the electronic alterations of the molecule in these excited states. Finally, we discuss the near-UV absorption spectrum of tubulin-bound colchicine and the implications of these results in understanding the nature of the environment of the colchicine-binding site on tubulin.

Experimental Procedures

Colchicine was obtained from Aldrich and used as supplied. Near-UV absorption spectra were measured on a Hewlett-Packard Model 8451A diode array spectrometer from 300 to 450 nm. Digitization of the spectra at 2-nm intervals was carried out by the spectrometer, and the digitized data were input into an IBM PC-AT for computer differentiation. The

† Current address: George R. Harrison Spectroscopy Laboratory, Massachusetts Institute of Technology, Cambridge, MA 02139.

(1) Fitzgerald, T. J. *Anti-Inflammatory Agents. Chemistry and Pharmacology*; Sherrer, R. A., Whitehouse, M. W., Eds.; Academic Press: New York, 1974; pp 295–361.
(2) Luduena, R. F. *Microtubules*; Roberts, K., Hyams, J. S., Eds.; Academic Press: New York, 1979; pp 66–116.
(3) Dustin, P. *Microtubules*, 2nd ed.; Springer-Verlag: New York, 1984.
(4) Shelanski, M. L.; Taylor, E. W. *J. Cell Biol.* **1968**, *38*, 304.
(5) Wiesenberg, R. C.; Borisy, G. G.; Taylor, E. W. *Biochemistry* **1968**, *7*, 4466.
(6) Bhattacharyya, B.; Wolff, J. *Proc. Natl. Acad. Sci. U.S.A.* **1974**, *71*, 2627.
(7) Garland, D. L. *Biochemistry* **1978**, *17*, 4266.
(8) Lambier, A.; Engelborghs, Y. *J. Biol. Chem.* **1981**, *256*, 3279.
(9) Detrich, H. W., III; Williams, R. C., Jr.; Macdonald, T. L.; Wilson, L.; Puett, D. *Biochemistry* **1981**, *21*, 5999.
(10) Andreu, J. M.; Timasheff, S. N. *Biochemistry* **1982**, *21*, 534.
(11) Andreu, J. M.; Timasheff, S. N. *Biochemistry* **1982**, *21*, 6465.
(12) Biswas, B. B.; Sen, K.; Choudhury, G. G.; Bhattacharyya, B. *J. Biosci.* **1984**, *6*, 431.
(13) Bhattacharyya, B.; Howard, R.; Maity, S. N.; Brossi, A.; Sharma, P. N.; Wolff, J. *Proc. Natl. Acad. Sci. U.S.A.* **1986**, *83*, 2052.
(14) Engelborghs, Y.; Fitzgerald, T. J. *J. Biol. Chem.* **1987**, *26*, 5204.
(15) Bane, S. Ph.D. Thesis, Vanderbilt University, 1983.
(16) Bhattacharyya, B.; Wolff, J. *J. Biol. Chem.* **1984**, *259*, 11836.
(17) Yeh, H. J. C.; Chrzanowska, M.; Brossi, A. *FEBS Lett.* **1988**, *229*, 82.

0002-7863/89/1511-6993$01.50/0

numerical method for obtaining the best signal to noise in the derivative spectra has been discussed by Butler and Hopkins[18] and is reviewed in the Appendix. Colchicine solutions (30 μM) were prepared in spectral-grade solvents, kept in the dark, and used within 1 h of preparation in order to preclude the possibility of photodecomposition.

Absorption spectra corresponding to dimerized colchicine were obtained in a manner similar to that described by Engelborghs.[19] The absorption spectrum of a 1 mM aqueous solution of colchicine was measured using a 0.1-cm cell, and the absorption spectrum of a 0.1 mM colchicine solution was measured using a 1.0-cm cell. A 25-s acquisition time was utilized in both measurements to reduce noise. Subtraction of the spectrum of the dilute from the concentrated solution yielded a difference spectrum that matched the previously published spectrum.[19] Since it has been shown that a 1 mM aqueous solution of colchicine is approximately 10% dimerized, the 1 mM spectrum was normalized to reflect the concentration of dimer and the 0.1 mM solution spectrum was subtracted to yield the absorption spectrum corresponding to the dimer. Derivatives of the dimer spectrum were accomplished in the usual manner.

Bovine brain tubulin, free of microtubule associated proteins, was prepared by two cycles of assembly/disassembly followed by phosphocellulose chromatography as described previously[20] and stored in liquid nitrogen. Tubulin obtained by this procedure is routinely >98% pure when analyzed by sodium dodecyl sulfate–polyacrylamide gel electrophoresis. Prior to use, the frozen pellets were gently thawed, centrifuged at 5000 × *g* for 10 min at 4 °C, and then desalted into PMEG buffer using 1-mL Sephadex G-50 columns according to the method of Penefsky.[21] (PMEG = 0.1 M PIPES, 1 mM $MgSO_4$, 2 mM EGTA, 0.1 mM GTP, pH 6.90 at 25 °C.) Tubulin concentrations were determined spectrophotometrically by the use of an extinction coefficient at 278.5 nm of 1.23 $(mL/mg)^{-1}$ cm^{-1} in PMEG buffer.[22] Colchicine (Aldrich) concentrations in aqueous solution were also determined spectrophotometrically using an extinction coefficient at 353 nm of 1.692×10^4 M^{-1} cm^{-1} in PMEG buffer.[15]

The colchicine–tubulin complex was formed by incubating equimolar concentrations of colchicine and tubulin at 37 °C for 90 min. After the incubation period, the colchicine–tubulin complex was separated from any unbound colchicine by gel filtration according to the method of Penefsky.[21] It is known that the isolated colchicine–tubulin complex is stable for several hours;[23] nonetheless, the absorption spectrum of the complex was recorded within 30 min after the gel filtration step.

Results and Discussion

A. Near-UV Absorption Spectrum of Colchicine in DMSO. In this section we discuss the near-UV spectrum of colchicine in DMSO. DMSO is chosen for initial discussion because the derivative spectra in this solvent illustrate the potential of derivative spectroscopy and contain all the information needed to understand the spectrum of colchicine. The near-UV visible absorption spectrum of colchicine in DMSO is shown in Figure 1a. The spectrum is broad and featureless with a maximum centered at approximately 340 nm. There may be some indication of a weak shoulder on the red side of the maximum, but this is difficult to detect. The second derivative of this spectrum is shown in Figure 1b. This derivative shows three distinct bands: a maximum negative band occurring at 342 nm correlating well with the absorption maximum observed and two smaller bands detected at 367 and 385 nm. A shoulder on the blue side of the major peak is also observed at 322 nm. The resolution of these bands is considerably enhanced in the fourth derivative spectrum (Figure 1c). The two bands at 385 and 367 nm are clearly resolved from the broad 342-nm band, and the 342-nm band is clearly shown to consist of two bands at 342 and 325 nm. Several additional bands can also be seen in the fourth derivative.

Two features of these derivative spectra need to be addressed: (1) the relative intensities of the 342-nm versus the 385- and 367-nm bands in the second and fourth derivatives, and (2) the assignment of the bands observed in the fourth derivative to

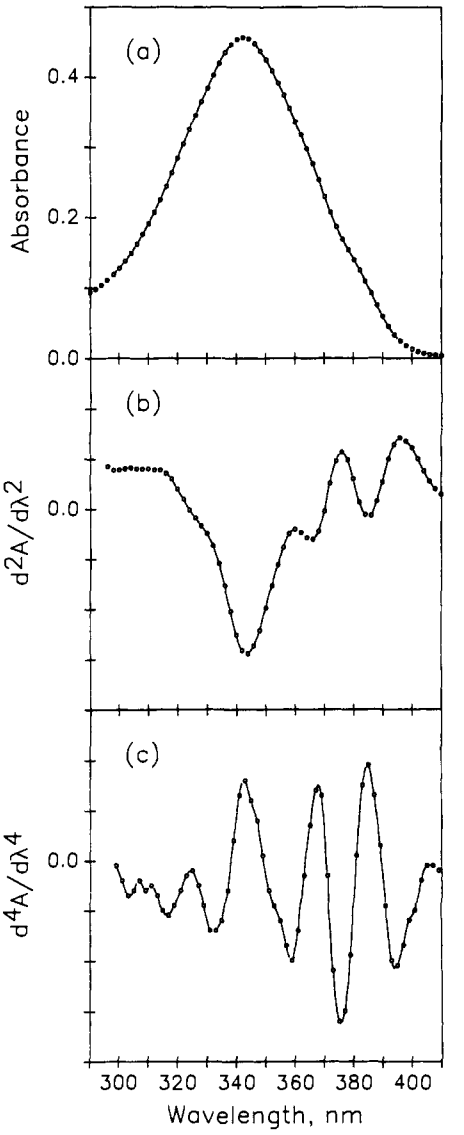

Figure 1. Absorption spectrum of colchicine in dimethyl sulfoxide and derivatives of the spectrum. (a) The absorption spectrum of colchicine in dimethyl sulfoxide (30 μM). (b) Second derivative of (a). (c) Fourth derivative of (a). Intensities in the derivative spectra are expressed in arbitrary units.

excited-state electronic levels of the colchicine. The 342-nm band has decreased intensity in the fourth derivative relative to the second derivative. The reason for the change in the relative intensity of this band on going from the absorption spectrum and second derivative to the fourth derivative is easily discerned from an understanding of the sensitivity of the higher order derivatives to bandwidth as discussed in the Appendix. The 342-nm band must have a larger bandwidth than the 385- and 367-nm bands, and thus the latter are preferentially enhanced in the higher derivatives. Other low-energy bands seem to follow the intensity of the latter while high-energy peaks correlate with the former.

Two possibilities might account for the increase in bandwidth (or decrease in excited-state lifetime) of the higher energy bands in the absorption spectrum. The first possibility is the molecule may gain additional nonradiative pathways from the excited state when high in the vibrational manifold, thus decreasing the lifetime with a consequent increase in the bandwidth.[24] This mechanism assumes there is only one excited state in this energy region. The second possibility seems more likely. The change in bandwidth and increase in intensity could be accounted for if the 342-nm

(18) Butler, W. L.; Hopkins, D. W. *Photochem. Photobiol.* **1970**, *12*, 439, 451.
(19) Engelborghs, Y. *J. Biol. Chem.* **1981**, *256*, 3276.
(20) Williams, R. C., Jr.; Lee, J. C. *Methods Enzymol.* **1982**, *85*, 376.
(21) Penefsky, H. S. *J. Biol. Chem.* **1977**, *252*, 2891.
(22) Detrich, H. W., III; Williams, R. C., Jr. *Biochemistry* **1978**, *17*, 3900.
(23) Sherline, P.; Lueng, J. T.; Kipnis, D. M. *J. Biol. Chem.* **1975**, *250*, 5481.
(24) Lakowicz, J. R. *Principles of Fluorescence Spectroscopy*; Plenum Press: New York, 1983.

Table I. Observed Fourth Derivative Absorption Bands of Colchicine in Different Solvents

solvent	ϵ^a	wavelength maxima, nm: low[b]		wavelength maxima, nm: high[c]		intensity of low/high[d]
dioxane	2.209	383	366	341	324	1.0
carbon tetrachloride	2.238	384	368	344	326	1.4
ethyl acetate	6.02	383	366	339	321	1.0
N,N'-dimethylformamide	37.65	385	367	341	323	1.1
dimethyl sulfoxide	44.8	385	367	342	323	1.2
methanol	32.63	380	362	340	*e*	2.2
ethanol	42.3	379	362	346	*e*	2.9
glycerol	42.5	382	360	341	*e*	3.9
water	80.37	382	362	338	*e*	2.7
formamide	109	381	363	342	*e*	2.0
tubulin (40 μM)		386	364	346	*e*	3.2
dimer[f]		382	367	342?[g]	*e*	

[a] Dielectric constant of the solvent. [b] Wavelength maxima of the pair of bands of the lower energy transition. [c] Wavelength maximum of the pair of bands of the higher energy transition. [d] Relative intensity of the peaks in the fourth derivative of the lower energy bands of the two transitions. Peak heights are measured from the abscissa to the peak maximum. [e] Too weak to be determined. [f] Second derivative wavelengths. [g] Difficult to determine precisely; see text.

band, and peaks to the blue, belong to a different excited state than the bands of lower energy. This would suggest that all the bands with smaller widths are vibrational structures of a low-energy, weak electronic transition and those with larger widths belong to a higher energy excited state with large oscillator strength and a shorter excited lifetime. This hypothesis is also supported by careful examination of the vibronic structure. The observed low-energy bands with narrower bandwidths are each approximately 1200-cm^{-1} apart, while the higher energy bands are about 1600 cm^{-1} from one another. The observation of separate vibrational progressions, each with its own distinctive Franck–Condon pattern, also suggests the existence of two excited states in this region of the absorption spectrum. We therefore conclude that the near-UV absorption band of colchicine is made up of two electronic transitions of different bandwidths. The lower energy excitation is highly structured, suggesting much vibronic activity, while the higher energy band is more diffuse.

B. Effect of Solvent. It is well-known that the character of a particular excited state can be determined by observing its behavior in solvents of different polarity and dielectric constant.[24,25] For example, the absorption band of an excited state that has a dipole moment greater than that of the ground state is shifted to longer wavelength (lower energy) in solvents of increasing polarity, while an excited state in which the dipole moment is less than the ground state is shifted to shorter wavelength in these solvents. Fluorescence bands are particularly sensitive to the dielectric constant of the medium, and this property can be used to distinguish fluorescence mechanisms. Additionally, specific interactions between solvent and solute such as hydrogen bonding will also affect the energy of the transition if electron density is shifted in the region of the hydrogen bond.

In the previous section we have shown that there must be two electronic transitions in the near-UV region to account for the structure in the second and fourth derivative of the absorption spectrum of colchicine in dimethyl sulfoxide (DMSO). In this section, the fourth derivative spectra are used to measure the peak positions of the two electronic transitions in different solvents, and the results are given in Table I. We will concentrate on the 362/382-nm (wavelengths in water) pair of bands first. These bands do not show a wavelength correlation with solvent polarity or other standard solvent parameters such as dipole moment or refractive index. However, the wavelengths of this pair of bands in the solvents capable of donating a hydrogen bond to the solute (ethanol, methanol, acetic acid, water, glycerol, and formamide) are consistently shifted to shorter wavelength (i.e., the excited-state levels are destabilized) 3–8 nm from their wavelengths in the non-hydrogen-bonding solvents. Assuming a hydrogen bond is formed on the carbonyl oxygen of the C ring, this result would suggest that the lowest energy transition involves movement of electron density away from the carbonyl region of the molecule. Such a wavelength shift might be expected for either an n–π^* excitation or a π–π^* charge-transfer-like transition, which transfers electron density from the carbonyl to the C ring. The extinction coefficient of the low-energy transition can be estimated from the overall absorption spectrum to be $\sim$1000 cm^{-1} M^{-1}. Since extinction coefficients of n–π^* excitations are generally at least 1 order of magnitude less than this value, it is reasonable to propose that this transition is π–π^* in nature.[6,26]

The behavior of the 341-nm band in different solvents is different from that observed for the lower energy transition. There is little apparent change in the energy of this transition regardless of the properties of the solvent. The intensity of this band, extinction coefficient of $\sim$5000 cm^{-1} M^{-1} in non-hydrogen-bonding solvents, does indeed suggest that the transition is due to a π–π^* excitation, although the nature of the transition is not entirely clear from the data. An assignment of the nature of this transition will require the results of the MNDO calculation.

The observation that the energies of the two transitions comprising the near-UV absorption band of colchicine are primarily affected by whether a solvent can be classified as non-hydrogen bond donating or hydrogen bond donating is also supported by the gross structural features of both the second and fourth derivative spectra. As demonstrated by the spectrum of colchicine in *N,N'*-Dimethylformamide (DMF; Figure 2), the high- and low-energy transitions are clearly distinguishable in the second and fourth derivative and are of approximately the same intensity in the fourth derivative in solvents that are incapable of hydrogen bond donation to the solute. Note however the decrease in the relative intensity of the higher energy transition in the fourth derivative of the absorption spectrum for methanol (Figure 3), a representative example of a hydrogen bond donating solvent, which has approximately the same dielectric constant as DMF (cf. Table I). Also note the apparent disappearance of the 360-nm band in the second derivative of the spectrum of colchicine in methanol even though the solvent does not affect the energy of the shorter wavelength band. The 2- to 3-fold decrease in intensity of the higher energy transition coupled with the shift to shorter wavelength of the low-energy transition leads to different characteristic second and fourth derivative spectra in hydrogn-bonding solvents.

Another feature that is clearly apparent in the hydrogen-bonding solvents is the appearance of an additional band in the fourth derivative spectrum at approximately 1700 cm^{-1} higher in energy than the longer wavelength band of the low-energy electronic transition. This band is likely due to an active vibronic level in the low-energy transition. The fact that it is found con-

(25) Suzuki, H. *Electronic Absorption Spectra and Geometry of Organic Molecules*; Academic Press: New York, 1967.

(26) Turro, N. J. *Modern Molecular Photochemistry*; Benjamin/Cummings: Menlo Park, CA, 1978; pp 103–109.

Table II. π-Electron Coefficients of the Carbon and Oxygen Atoms of Tropone As Determined by MNDO

		atom no.[a]							
orbital	energy, eV	1	3	4	5	6	7	8	9
LUMO + 1	−0.42	−0.41	0.44	0.21	−0.46	0.22	0.14	−0.49	0.29
LUMO	−1.05	−0.04	0.03	0.48	−0.30	−0.44	0.48	0.22	−0.45
HOMO	−9.08	0.37	−0.02	−0.44	−0.23	0.43	0.42	−0.24	−0.44
HOMO − 1[b]	−10.68	−0.84	0.16	−0.27	0.06	0.00	−0.01	0.08	−0.29
HOMO − 2	−10.86	0.02	0.00	−0.45	−0.51	−0.16	0.17	0.52	0.45

[a] Numbers refer to the atom numbering schemes in Figure 4. [b] p_x orbital coefficients.

sistently 1700 cm^{-1} from what appears to be the 0–0 band indicates that a reasonable assignment would be a carbonyl stretching vibrational mode. It is likely that the additional intensity of this vibration in hydrogen-bonding solvents is due to the dipole induced by a hydrogen bond in the carbonyl region of the molecule.

C. **MNDO Calculations.** The experiment yields observations about the relative energies of the different components of a complicated absorption band using derivative techniques. It would be difficult, however, to relate these observations to the many possible transitions that might take place in a molecule the size of colchicine and to decide the main character of the observed transitions. In order to do so, we have undertaken MNDO calculations of the ground-state molecular orbitals of colchicine and tropone (as a model for the low-energy transitions).[27] These calculations were carried out on an IBM PC AT equipped with an OASYS 32-bit system running UNIX. It is not our intention to gain a quantitative picture of the electronic excited states of this molecule, which might be available with extensive molecular orbital treatments and configuration interaction; rather, we wish to gain an intuitively useful understanding of the types of low-energy transitions available to colchicine.

1. Tropone. Tropone is initially considered as a model for the electronic transitions that may occur in the C ring of colchicine. With an angle of 54° indicated by the X-ray crystal structure of colchicine,[28,29] it would be expected that conjugation of the C ring with the π-system of the A ring would not be important to the possible electronic transitions, and thus this molecule should serve as a good paradigm. Extended Hückel calculations have been performed previously on tropone, which indicated that the n–π^* transition from the lone pair on the carbonyl oxygen may play a role in the observed absorption spectra of the colchicinoids.[30]

MNDO calculations on tropone have been carried out using the X-ray crystal structure geometry.[31] The energies and coefficients of the p_z atomic orbitals for the two π-orbitals HOMO (H) and LUMO (L), and the two π-orbitals energetically below and above the HOMO and LUMO, HOMO−2 (H−2) and LUMO+1 (L+1), are given in Table II with the atom numbering indicated on the colchicine structure of Figure 4. Also given in Table II is the energy and coefficients of the p_x HOMO−1 (H−1) orbital, which is effectively the nonbonding orbital of the carbonyl oxygen.

The calculation indicates that the energy of the nonbonding orbital is significantly lower than that of the π HOMO orbital. In addition, the energies of the L and L+1 orbitals are relatively close, particularly when compared to the energy difference between H and H−1. Thus the two lowest energy transitions of tropone from the orbital point of view would be expected to consist primarily of H → L and H → L+1 character, and both would be π–π^* type transitions. This result is in agreement with the observed high extinction coefficients of the two near-UV transitions of colchicine and would seem to confirm that the n–π^* transition is not playing an important role in the near-UV absorption spectrum of the tropone ring. We have not carried out configuration interaction, which would alter the overall quantitative energies of the π–π^* and n–π^* electronic states, but in view of the large energy differences calculated between the π- and n-orbitals we would not expect configurational interaction to alter the qualitative picture being discussed here.

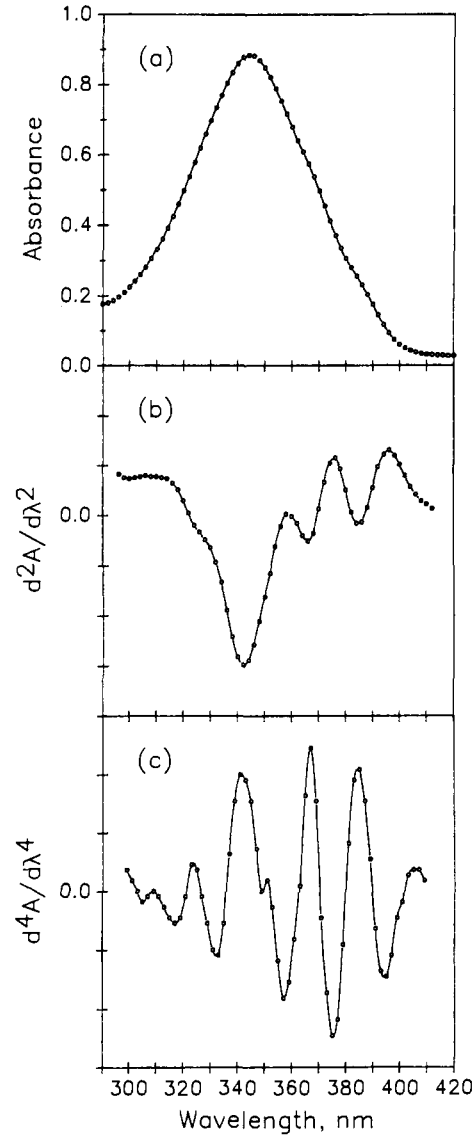

Figure 2. Absorption spectrum of colchicine in *N,N'*-dimethylformamide and derivatives of the spectrum. The absorption spectrum of 50 μM colchicine in DMF is shown in (a). The spectra in (b) and (c) are the second and fourth derivatives, respectively, of the spectrum in (a). The amplitudes of the second and fourth derivative spectra have been scaled for clarity.

We therefore conclude that the two lowest energy transitions in the tropone moiety are indeed π–π^* in nature and very close in energy. Consider the symmetry of each of the orbitals H, L, and L+1 involved in these transitions. If we assume that the overall symmetry of tropone sufficiently approximates C_{2v}, then the symmetry of H, L, and L+1 are b_2, a_1, and b_2, respectively. The H → L configuration is therefore of b_2 symmetry and the H → L+1 configuration is of a_1 symmetry. The two transitions are thus not allowed to mix by configuration interaction and should result in two separate distinguishable absorption bands.

(27) Dewar, M. J. S.; Thiel, W. *J. Am. Chem. Soc.* **1977**, *99*, 4899.
(28) Margulis, T. N. *J. Am. Chem. Soc.* **1974**, *96*, 899.
(29) Lessinger, L.; Margulis, T. N. *Acta Crystallogr.* **1978**, *B34*, 578.
(30) Yamaguchi, Y.; Amako, Y.; Azumi, H. *Tetrahedron* **1967**, *24*, 267.
(31) Barrow, M. J.; Mills, O. S. *J. Chem. Soc., Chem. Commun.* **1973**, 66.

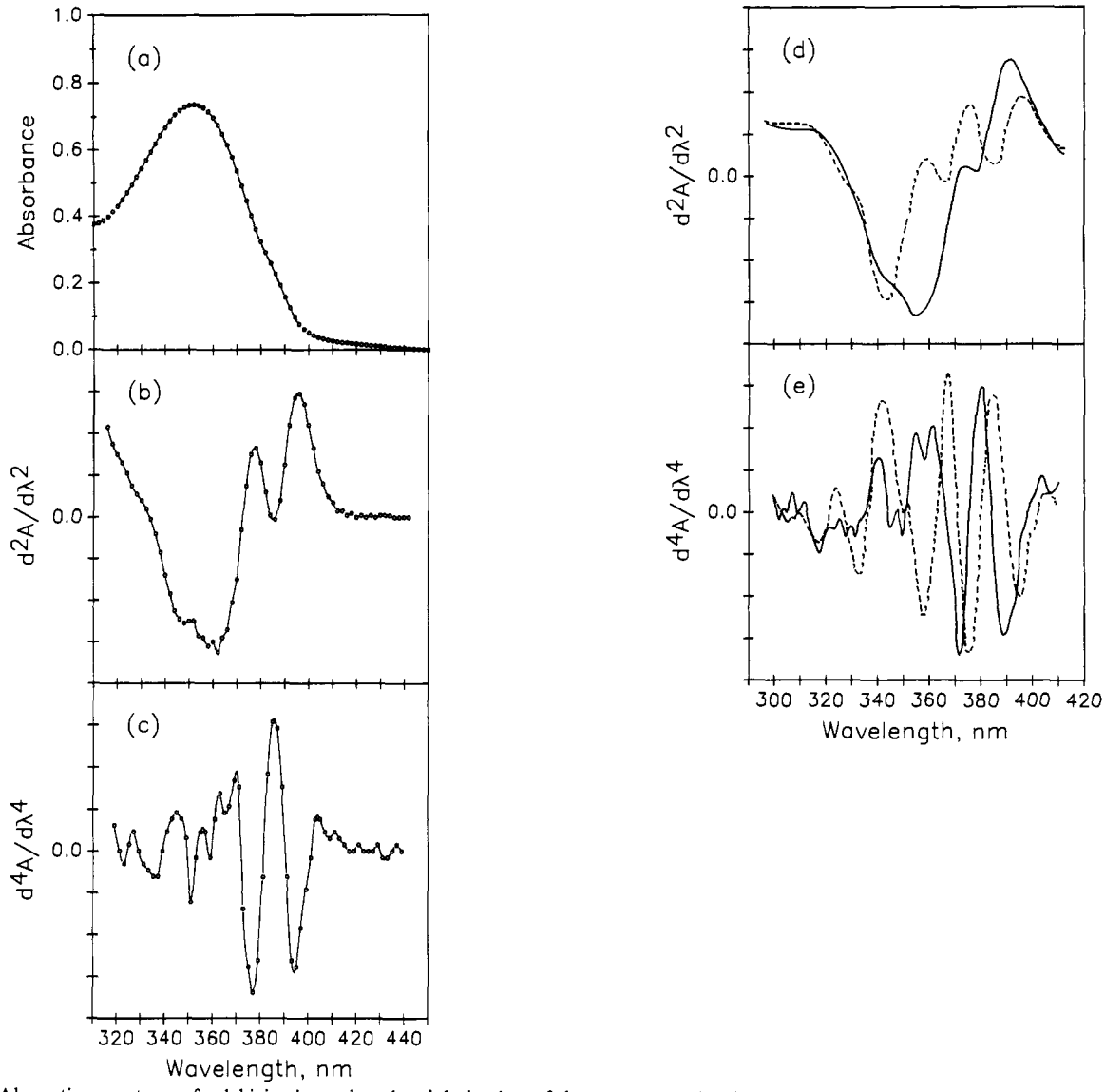

Figure 3. Absorption spectrum of colchicine in methanol and derivatives of the spectrum. The absorption spectrum of 50 μM colchicine in methanol is shown in (a). The second and fourth derivatives of (a) are shown in (b) and (c), respectively. The amplitudes of the derivative spectra have been scaled for clarity. In (d) and (e) the second and fourth derivative spectra of colchicine in *N,N'*-dimethylformamide (dashed line) and methanol (solid line) are overlaid for comparison.

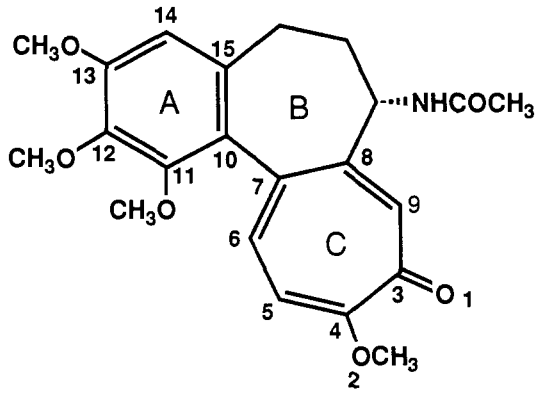

Figure 4. Structure of colchicine. The atom numbers refer to the numbering for MNDO calculations (Tables II–IV). Letters refer to the conventional designation of the rings.

The change in electron density in these two electronic configurations should also be consistent with the behavior found for each of the transitions in different solvents. We observed above that the long wavelength bands in colchicine are shifted to shorter wavelength in hydrogen-bonding solvents, a result which is considered unusual for a π–π^* excitation. The π-electron coefficients shown in Table II for the H, L, and L+1 orbitals show that π-electron density has moved away from the carbonyl oxygen into the seven-membered ring for the H $\rightarrow$ L configuration (see atom 1 in Table II). Thus, a hydrogen bond formed in the ground state would destabilize the L orbital and raise its energy in hydrogen-bonding solvents, which is in agreement with the experimental observations. The H $\rightarrow$ L+1 excitation results in a small increase in the π-electron density at the carbonyl oxygen, and therefore a small shift to longer wavelength might be expected in hydrogen-bonding solvents. The change in the π-electron density, however, is quite small and may not be experimentally observable.

2. Colchicine. The coefficients of the p_z orbitals and energies for the H, L, and L+1 molecular orbitals of colchicine are given in Table III. These are calculated using the geometry of colchicine obtained from X-ray crystal studies.[28] Several observations about these orbitals are important. First, between 70 and 90% of the total electron density in these molecular orbitals can be accounted for by the tropone moiety; thus, the lowest energy transitions of the colchicine are localized primarily on the tropone portion of the molecule. Second, except for small perturbations in the magnitudes of the coefficients, the tropone portions of these orbitals mimic those orbitals found in tropone. The lowest energy transitions in colchicine therefore maintain much of the C_{2v} symmetry

Table III. π-Orbital Coefficients for Molecular Orbitals Determined from MNDO for the X-ray Crystal Structure of Colchicine

		atom no.[a]														
orbital	energy, eV	1	2	3	4	5	6	7	8	9	10	11	12	13	14	15
LUMO+1	−0.69	0.40	0.04	−0.41	−0.08	0.30	−0.22	−0.08	0.53	−0.35	−0.07	0.03	0.02	−0.06	0.03	0.04
LUMO	−1.07	0.09	0.18	−0.08	−0.48	0.25	0.41	−0.39	−0.15	0.31	−0.12	0.07	0.04	−0.12	0.03	0.09
HOMO	−8.67	−0.26	−0.25	0.03	0.33	0.31	−0.32	−0.41	0.06	0.27	0.18	0.06	−0.08	−0.13	−0.07	0.08
HOMO−1	−9.46	−0.13	−0.14	0.00	0.15	0.18	−0.05	−0.17	0.06	0.14	−0.20	0.10	0.30	0.18	0.01	−0.25

[a] Numbers refer to atom numbering scheme in Figure 4.

Table IV. π-Orbital Coefficients for Molecular Orbitals Determined from MNDO for the 19° Conformation of Colchicine

		atom no.[a]														
orbital	energy, eV	1	2	3	4	5	6	7	8	9	10	11	12	13	14	15
LUMO+1	−0.56	−0.12	−0.08	0.12	0.21	−0.18	−0.08	0.18	0.04	−0.05	−0.04	−0.42	0.40	0.08	−0.44	0.23
LUMO	−1.16	0.11	0.15	−0.09	−0.41	0.20	0.40	−0.32	−0.03	0.21	−0.31	0.09	0.21	−0.26	−0.04	0.24
HOMO	−8.31	−0.25	−0.23	0.03	0.33	0.28	−0.35	−0.40	0.08	0.27	0.25	0.14	−0.13	−0.23	−0.08	0.18
HOMO−1	−9.35	0.13	0.13	0.01	−0.14	−0.19	0.04	0.17	−0.09	−0.14	0.23	−0.29	−0.43	−0.16	0.20	0.27

[a] Numbers refer to atom numbering scheme in Figure 4.

of the tropone moiety and their sensitivity to solvent perturbations. Finally, the benzene moiety of the A ring makes little or no contribution to the character of the lowest energy configurations.

The energy of the nonbonding orbital of the carbonyl oxygen of the C ring in colchicine remains about 1.4 eV below that of the H orbital, similar to the result found in tropone. In contrast to tropone, however, there are three obitals between the n and H orbital, consisting of mainly A ring π-character. Transitions from the nonbonding orbital are therefore not expected to be important to the near-UV absorption band of colchicine.

D. Absorption Spectrum of Colchicine Bound to Tubulin. The absorption spectrum of tubulin-bound colchicine and its second and fourth derivatives are shown in Figure 5. There are several features of the spectrum that should be noted. Careful examination of the spectrum reveals that the energies and the intensities of the bands cannot be directly explained by either invoking a hydrogen-bonding or non-hydrogen-bonding environment. This result is not entirely unexpected, as the spectral characteristics related to the electronic properties of the molecule (fluorescence, CD) have never been precisely duplicated under any experimental conditions to date in the absence of tubulin. The bands corresponding to the low-energy transition are found at 364 and 386 nm, which is the same region in which the low-energy transition is found in non-hydrogen-bonding solvents. These results are consistent with the idea that the colchicine-binding site on tubulin is a hydrophobic pocket in the protein, analogous to other protein-binding sites for ligands with extended π-systems. Note, however, the relative intensity of this pair of bands and the 346-nm band in the fourth derivative (Figure 5c and Table I). These bands are decreased in intensity relative to the higher energy transition, which is similar to the effects observed in hydrogen-bonding solvents. Furthermore, the high-energy transition is shifted to longer wavelength relative to its energy observed in all solvents examined. Thus, the derivatives of the electronic spectrum of colchicine bound to tubulin confirm observations that the electronic nature of the molecule is altered in a unique manner upon tubulin binding.

There are several mechanisms that might account for the altered electronic character. The first is the proposed conformational change in the molecule upon binding to tubulin, which is expected to change the angle between the A and C rings from 54° to 19°.[9] In order to evaluate the effects of such a geometry change on the molecular orbitals, MNDO calculations of the ground-state molecular orbitals in which the angle between the two rings was reduced to 19° were undertaken (Table IV). The calculations indicate that the H and L orbitals are very similar in character to the 54° conformation, but the difference in energy between H and L has decreased by ~0.5 eV, which would result in a 50-nm shift to longer wavelength of the low-energy transition. In addition, the L+1 orbital is now localized on the A ring; thus, the short wavelength band would also be greatly altered. This analysis coupled with the observation that the overall features in the tubulin-bound colchicine absorption spectrum are similar to the molecule free in solution would seem to preclude the significant

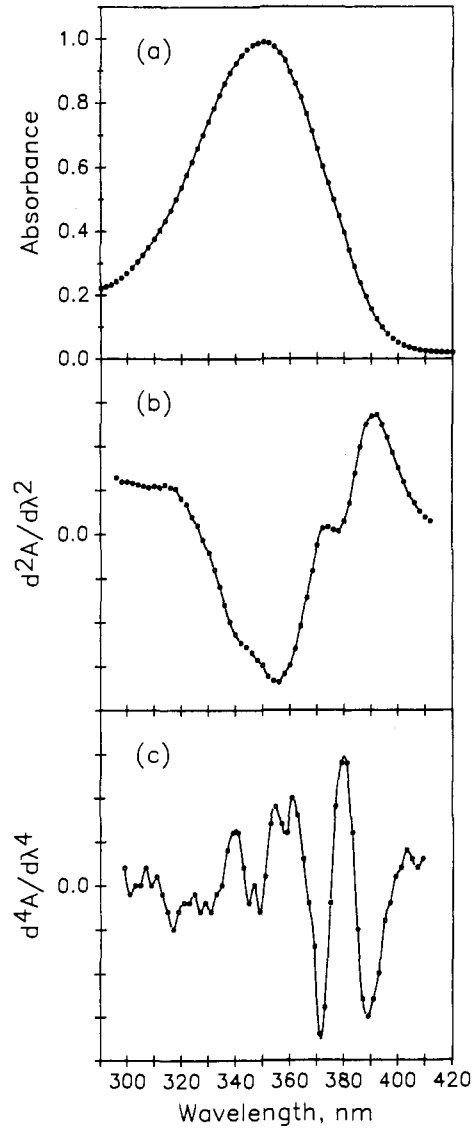

Figure 5. Absorption spectrum of colchicine bound to tubulin and derivatives of the spectrum. The absorption spectrum of 40 μM tubulin–colchicine complex in PMEG buffer at ambient temperature is shown in (a). The colchicine–tubulin complex was prepared as described in the text. The second and fourth derivatives of (a) are shown in (b) and (c), respectively. The amplitudes of the derivative spectra have been scaled for clarity.

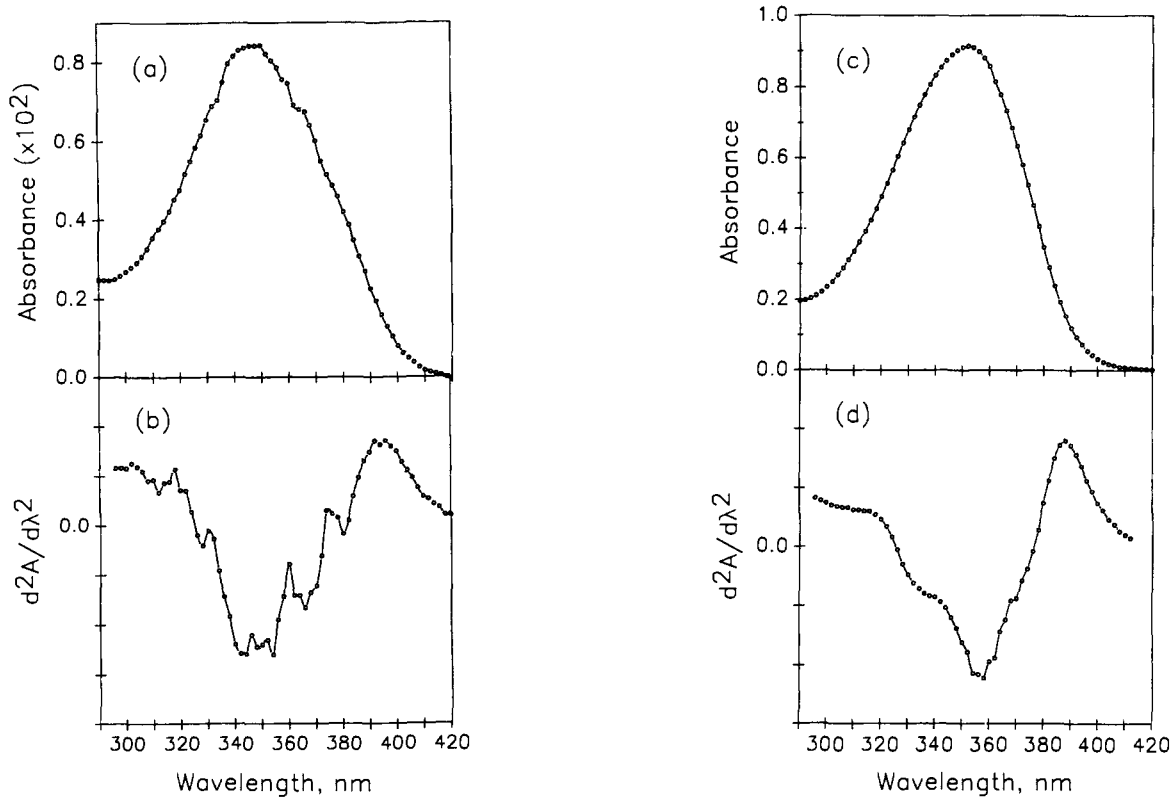

Figure 6. Absorption spectrum and second derivative of the spectrum of colchicine and colchicine dimer in water. The absorption spectrum in (a) in the spectrum of dimerized colchicine, obtained from a 1 mM aqueous solution as described in the text. The second derivative of (a) is shown in (b). The spectra in (c) and (d) are the absorption and second derivative spectra of an aqueous solution of colchicine (50 μm) in which no detectable dimerization is present. The amplitudes of the second derivative spectra are expressed in arbitrary units.

conformational change previously suggested.

A second explanation for the altered electronic spectrum of the bound ligand could invoke an overall apolar binding site (causing the observed shift in the long wavelength bands) in which a localized hydrogen bond to the methoxy group oxygen of the C ring exists, which might cause the shift to long wavelength in the short wavelength band. (A hydrogen bond to the carbonyl oxygen would have been indicated by a shift to short wavelength in the low-energy bands.) The MNDO calculations indicate that the H and L orbitals have similar electron density on the methoxy group oxygen, and thus a hydrogen bond would not alter the energy of the long wavelength bands. But the L+1 has significantly decreased electron density (see Table III). A hydrogen bond at this position would destabilize the energy of the L+1 orbital causing a shift to *short* wavelength in the observed spectrum. This is clearly not supported by the experimental data.

A third mechanism that might explain the tubulin-bound spectrum is the interaction of the colchicine C ring π-system with a π-system within the colchicine binding site. Such an interaction might cause the observed hypochroism in the high-energy band and consequent wavelength shift. In order to determine if π-interactions might be able to account for the features in the observed derivative spectra, we undertook a study of the colchicine dimer in aqueous solution (1 mM) that is believed to undergo π-stacking. An absorption spectrum of the pure dimer, obtained as described in Experimental Procedures, is shown in Figure 6. The second derivative of this spectrum (Figure 6b) shows features at 383 and 368 nm, corresponding to the low-energy bands seen in the free colchicine spectra observed in non-hydrogen-bonding solvents and completely different from the monomer colchicine spectrum in aqueous solution (parts c and d of Figure 6). The energies of the bands indicate that the carbonyl region of the dimer is not hydrogen bonded in spite of the fact that this molecule is in aqueous solution.

It is difficult to determine if the position of the higher energy transition is shifted to the long wavelength in the dimer as it is in tubulin. The second derivative indicates a maximum negative band at 342 nm though the center of this band is at 346 nm, similar to the result of the bound colchicine. It is not possible to analyze the fourth derivative because of the increased noise inherent in the difference spectrum. The relative intensity of the short wavelength bands to the long wavelength bands in the second derivative, however, is greater than that found for the tubulin-bound species.

It is important to point out that the dimer spectrum should not necessarily exactly mimic the spectrum of the tubulin-bound species. A π-system of the protein with which the colchicine π-system would interact would not be the same as the π-interactions of colchicine with itself. The colchicine dimer need not interact by a complete stacking since π-overlap of only the C ring of the molecule could preclude the hydrogen bond in aqueous solution. Similar interactions of the carbonyl region of the C ring with a π-region of the protein might cause the observed electronic changes. Nonetheless, the observed similarities between the second derivative spectra of the dimer and the tubulin-bound species would suggest π-stacking as a mechanism by which alteration of the electronic properties of the bound molecule may occur. This mechanism would also be consistent with the inability to mimic the electronic alterations of the bound species with simple solvent effects.

Conclusions

Study of the near-UV absorption spectrum of colchicine in different solvents utilizing multiple differentiation indicates two π–π^* excited states of different electronic characteristics. MNDO calculations confirm that the lower energy bands result from an excitation to an orbital which possesses little electron density on the carbonyl portion of the C ring. The higher energy transition results in a small increase in dipole moment. n–π^* excitations are found to be unimportant in the observed spectrum.

Analysis of derivative spectra of colchicine bound to tubulin indicates that the colchicine-binding site on tubulin is overall apolar in nature. These spectra also reveal the precise manner in which the electronic transitions of colchicine are altered upon tubulin

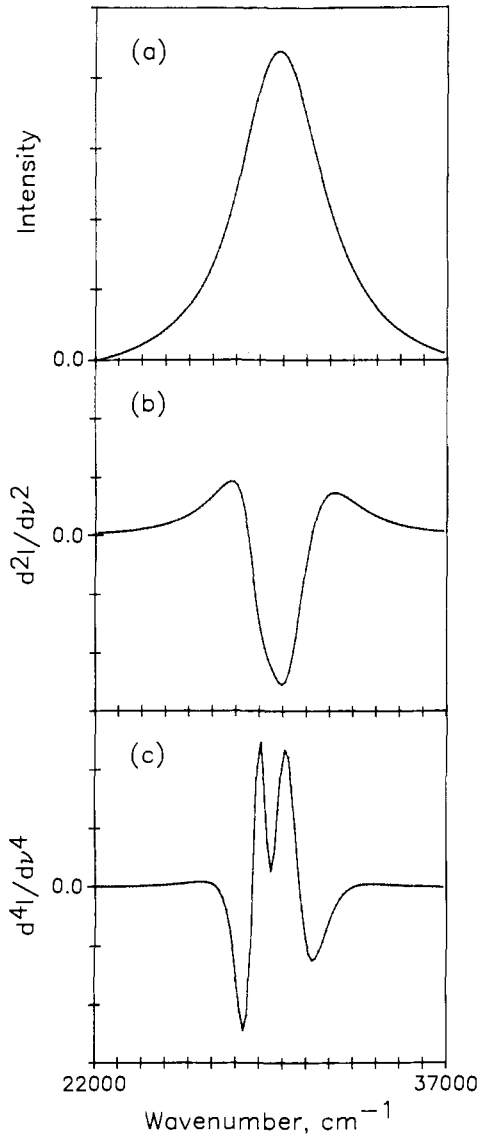

Figure 7. (a) An absorption spectrum generated from the sum of two Lorentzian bands with parameters $\nu_0 = 30000$ cm^{-1}, $b = 2200$ cm^{-1}, and $a/b^2 = 100$ and $\nu_0 = 29000$ cm^{-1}, $b = 1200$ cm^{-1}, and $a/b^2 = 10$. (b) Second derivative of (a). (c) Fourth derivative of (a). The amplitudes of the spectra have been scaled for clarity.

binding, which are unique to complex formation; i.e., the higher energy transition undergoes hypochroism and is shifted to longer wavelength when bound to the protein. The small magnitude of the bathochromic shift in this transition coupled with the results from MNDO calculations argue against a major conformational change in colchicine as accounting for the alteration in the electronic properties in the tubulin-bound species. A binding site environment, which is overall apolar but donates a hydrogen bond to a C ring oxygen, is also not supported by theoretical or experimental results. A mechanism that is consistent with both the experiment and theory is one in which a π-system of the protein is in close enough proximity to the colchicine C ring to perturb the electronic transitions of the ligand. The hypochroism caused by such an interaction in the high-energy transition might also account for the disappearance of the CD band. Confirmation of this mechanism awaits study of the absorption spectra of other colchicinoids.

Acknowledgment. This research was supported by an Accelerated Research Initiation Award from the Research Foundation, State University of New York, University Center at Binghamton (R.P.R. and S.B.H.) and by a BRSG grant (S07RR08149-15) awarded by the Biomedical Research Grant Program Division of Research Resources, National Insitutes of Health (S.B.H.). We thank Renee M. Chabin for her assistance in collecting the data and Robzens for providing bovine brains.

Appendix

A. Theoretical Background. Discussion of the applicability of derivatives to separate close-lying absorption bands has been noted in the literature, and the general band shapes expected for the individual derivatives have been throughly analyzed. In this appendix we concentrate on the practicality of the derivatives to distinguish between overlapping bands of unequal bandwidths differing by 30–50%. This possibility has not been explicitly demonstrated. In particular, we will focus on the second and fourth derivatives to discriminate between bands of disparate bandwidth.

A typical absorption band is considered, which has a Lorentzian band shape give by

$$I(\nu) = a/\{(\nu - \nu_0)^2 + b^2\} \quad \text{(A1)}$$

where ν_0 is the center frequency of the band (cm^{-1}), b is the width at half the maximum intensity (cm^{-1}), and a/b^2 is the peak intensity.[32] A real absorption band may have some Gaussian character and/or is equally well represented by an expansion in polynomials, but our conclusions based on the Lorentzian band shape are consistent with the experimental results. Only the second and fourth derivatives will be considered since these derivatives, and other even derivatives, can be shown to contain peak minima or maxima at ν_0.

The second derivative of a Lorentzian absorption band is given by

$$I''(\nu) = -2a\{b^2 - 3(\nu - \nu_0)^2\}/\{[(\nu - \nu_0)^2 - b^2]^3\} \quad \text{(A2)}$$

It should be noted from eq A2 that the second derivative will show negative peaks with maximum intensity $2a/b^4$. Whereas the intensity of the original absorption spectrum was proportional to $1/b^2$, the second derivative intensity is proportional to $1/b^4$. The half-width of the negative part of the second derivative can be shown to be 0.326 times that of the original. Similarly, the fourth derivative given by

$$I''''(\nu) = 24ab^2\{b^2 - 10(\nu - \nu_0)^2 + 5(\nu - \nu_0)^4/b^2\}/\{[(\nu - \nu_0)^2 + b^2]^5\} \quad \text{(A3)}$$

shows positive bands with maximum intensity $24a/b^6$, and the intensity is proportional to $10b^6$. The half-width of the positive part of the fourth derivative band is 0.208 times that of the original band.

It is instructive to compare the overlap of two Lorentzian bands with slightly different bandwidths. Figure 7a shows a theoretical absorption band generated by the addition of two Lorentzian bands with $\nu_0 = 30000$ cm^{-1}, $a/b^2 = 100$, and $b = 2200$ cm^{-1} and $\nu_0 = 29000$ cm^{-1}, $a/b^2 = 10$, and $b = 1200$ cm^{-1}. The spectrum is featureless, containing no indication of the weaker low-energy band. The asymmetry in the second derivative (Figure 7b) indicates the possible presence of a weaker peak. This weak band might be interpreted as a vibronic shoulder of the major peak if measurements are discontinued at this point. The fourth derivative (Figure 7c), however, shows the lower energy band with equivalent intensity to the higher energy band. The change in intensities between the second and fourth derivative occurs because of the dependence on width of the derivatives. This technique can thus be used to discriminate between bands of disparate widths and/or to enhance weaker peaks, which have narrower bandwidths. Significant changes in the relative intensities of individual bands in different derivatives can usually be taken to indicate that the separate bands belong to different electronic transitions.

B. Obtaining the Necessary Signal to Noise. A common misconception is that higher order derivatives of absorption spectra

(32) Madams, W. F. *Makromol. Chem., Macromol. Symp.* **1986**, *5*, 35, and references therein.

have insufficient signal to noise to carry out a spectral interpretation. In this section we address two ways in which this difficulty is overcome in our work.

The first consideration is the instrument on which absorption spectra are obtained. In a normal scanning instrument, every wavelength point is subject to random noise generated during the time the spectrometer is tuned to that particular wavelength. The result is a low-intensity but high-frequency noise that may be convoluted on an absorption spectrum. Although this noise may not be an important problem in monitoring the pure absorption spectrum, as demonstrated above, peaks with smaller bandwidths are enhanced greatly in the higher order derivatives. Thus, noise and its associated small bandwidth will be greatly enhanced. Our spectra have been obtained with a diode array absorption spectrometer, however, and this high-frequency noise is eliminated since the spectrum is not collected from point to point. All wavelengths are collected simultaneously. The availability of these detection systems is the primary reason higher order derivatives of absorption spectra can be obtained.

The numerical methods chosen to find derivatives are also an important consideration in establishing the signal to noise. Derivatives were carried out using the techniques described by Butler and Hopkins.[18] These authors showed both experimentally and theoretically that the up to 4 times enhancement in the signal to noise of the derivative spectra could be obtained by careful consideration of the derivative intervals. Specifically for a linear array, the fourth derivative intervals should differ by 2, 1, 1, and 1 intervals. For example, in our spectra, which are digitized at 2-nm intervals, the first derivative is taken for differences every 10 nm (5 "intervals"), the second every 6 nm (3 "intervals"), the third every 4 nm (2 "intervals"), and the fourth every 2 nm (1 "interval"), leading to the 2, 1, 1, and 1 interval differences needed for the best signal to noise.

With the combination of the diode array absorption spectrometer and the Butler/Hopkins numerical method, derivatives could be obtained directly from the data. No data smoothing was found to be necessary, and more than sufficient signal to noise was obtained.

Concerning the Crystal Structure of Porphine: A Proton Pulsed and ^{13}C CPMAS NMR Study

Lucio Frydman,[†] Alejandro C. Olivieri,[†] Luis E. Diaz,[†] Benjamin Frydman,*[,†] Irina Kustanovich,[‡] and Shimon Vega[‡]

Contribution from the Facultad de Farmacia y Bioquimica, Universidad de Buenos Aires, Junin 956, 1113 Buenos Aires, Argentina, and the Department of Isotope Research, The Weizmann Institute of Sciences, 76100 Rehovot, Israel. *Received May 31, 1988*

Abstract: Solid-state NMR techniques were employed in order to study the structure and the dynamics of porphine. The changes observed in the line width of the ^1H NMR signal between 173 and 443 K suggest that the porphine macrocycles rotate in the crystals. This was confirmed by recording the ^{13}C CPMAS NMR spectra at different temperatures which showed, in addition to the expected coalescence of signals due to the central hydrogens tautomerism, a broadening of the resonances due to the overall molecular rotation. These studies, coupled to measurements at different temperatures and fields of the relaxation times of the ^1H magnetization in the rotating frame, allowed us to obtain activation parameters for the motion which are, within experimental error, equal to those made available by CPMAS NMR for the tautomerism of the central hydrogens. These results suggest an explanation for what seems to be a contradiction between the structure of porphine observed by X-ray, according to which the central hydrogens are localized in opposite pairs of nitrogens, and the structure observed by CPMAS in which the hydrogens migrate between the four central nitrogens. If it is assumed that the migration of the central hydrogens is coupled to a 90° rotation of the molecules, the translational symmetry of the crystal will not be changed by the tautomerism, and an X-ray analysis would always detect a single tautomer.

Free-base porphyrins possess two inner hydrogens bonded to opposite pairs of nitrogen atoms. Since there are four such atoms in porphyrins, the central hydrogens can jump between two different configurations (Figure 1) giving rise to a tautomeric process which has been extensively studied by ^1H, ^{13}C, and ^{15}N variable-temperature solution NMR both in symmetrically[1-12] as well as in asymmetrically[13-15] substituted porphyrins. These studies have shown that in the former molecules, the hydrogens migrate in an effective double minimum potential between two equally populated tautomers A and B with a rate which at room temperature is fast on the NMR time scale (ca. 10^3 Hz). The tautomeric behavior of these free-base porphyrins has also been recently explored in the solid state by means of ^{13}C and ^{15}N CPMAS NMR,[16-20] where it was found that the symmetry of the double minimum potential may be perturbed by the crystal packing forces. Nevertheless in at least two porphyrins, *meso*-tetratolylporphyrin and porphine, the kinetic behavior of the central hydrogens in the solid state was found to be similar to the one

[†] University of Buenos Aires.
[‡] The Weizmann Institute of Sciences.

(1) Storm, C. B.; Teklu, Y. *J. Am. Chem. Soc.* **1972**, *94*, 1745.
(2) Abraham, R. J.; Hawkes, G.; Smith, K. *Tetrahedron Lett.* **1974**, 1483.
(3) Eaton, S. S.; Eaton, G. R. *J. Am. Chem. Soc.* **1977**, *99*, 1601.
(4) Gust, D.; Roberts, J. D. *J. Am. Chem. Soc.* **1977**, *99*, 3637.
(5) Yeh, H. J. C.; Sato, M.; Morishima, I. *J. Magn. Reson.* **1977**, *26*, 365.
(6) Limbach, H.-H.; Hennig, J. *J. Chem. Soc., Faraday Trans II* **1979**, *75*, 752.
(7) Limbach, H.-H.; Hennig, J. *J. Chem. Phys.* **1979**, *71*, 3120.
(8) Limbach, H.-H.; Hennig, J.; Gerritzen, D.; Rumpel, H. *Faraday Discuss. Chem. Soc.* **1982**, *74*, 229.
(9) Limbach, H.-H.; Hennig, J.; Stulz, J. *J. Chem. Phys.* **1983**, *78*, 5432.
(10) Hennig, J.; Limbach, H.-H. *J. Am. Chem. Soc.* **1984**, *106*, 292.
(11) Stilbs, P.; Moseley, M. E. *J. Chem. Soc., Faraday Trans. II* **1980**, *76*, 729.
(12) Stilbs, P. *J. Magn. Reson.* **1984**, *58*, 152.
(13) Crossley, M. J.; Harding, M. M.; Sternhell, S. J. *J. Am. Chem. Soc.* **1986**, *108*, 3608.
(14) Crossley, M. J.; Field, L. D.; Harding, M. M.; Sternhell, S. J. *J. Am. Chem. Soc.* **1987**, *109*, 2335.

0002-7863/89/1511-7001$01.50/0